Tuijin Jishu/Journal of Propulsion Technology
ISSN: 1001-4055
Vol. 44 No. 5 (2023)

Lorentz force and viscous dissipation consequences convective flow of a hybrid nanofluid with different base fluids in heat transfer over a stretching sheet

(A Subashini[1] , Dr R Lakshmi[2])

[1]Research scholar, Department of Mathematics, PSGR Krishnammal College for Women, Coimbatore – 641004, Tamil Nadu, India.
[2]Assistant Professor, Department of Mathematics, PSGR Krishnammal College for Women, Coimbatore – 641004, Tamil Nadu, India.

Abstract : Hybrid nanofluids have grown important consideration in modern centuries due to their greater thermal and rheological characteristics compared to conventional nanofluids. The primary goal of this research is to provide more details on the stable and incompressible stream of a hybrid nanofluid over a stretching sheet in two dimensions and the same is to be investigated. In the hybrid nanofluid flow, which consists of TiO_2 and Cu as nanoparticles, (H_2O, and $NaC_6H_9O_7$) are considered as base fluids. Additionally, consideration is given to the components of the magnetic field and viscous dissipation. Prior to being solved numerically using the Runge-Kutta fourth-order method, the existing partial differential equations are first transformed into ordinary differential equations using similarity transformations. The results illustrate that significant parameter such as the magnetic parameter, nanoparticles of solid volume fractions, Eckert number, and Casson parameter significantly influence momentum and thermal profiles. These analyses protest that raising the Eckert number grounds an increase in the hybrid nanofluid temperature. Moreover, the Casson parameter has decreased the temperature profile in TiO_2-Cu/ sodium alginate hybrid nanofluids. One of the promising applications of hybrid nanofluids is the heat transmission enhancement for a stretching sheet.

Keywords: Stretching sheet, Lorentz force, viscous dissipation, hybrid nanofluid.

Nomenclature

C_f	skin friction coefficient
C_p	specific heat, $jkg^{-1}k^{-1}$
k	thermal conductivity, $wm^{-1}k^{-1}$
M	magnetic parameter
Nu_x	local Nusselt number
Pr	Prandtl number
q_w	surface heat flux, wm^{-2}
Ec	Eckert number
T	temperature of fluid
T_w	ambient thermal
T_∞	surface thermal
u_w	constant velocity,

u, v	momentum factor in the x way
Greek letters	
β	Casson parameter
ϕ_{np1} , ϕ_{np2}	nanoparticles of volume fraction
μ	dynamic viscosity, $kgm^{-1}s^{-1}$
υ	kinematic viscosity, m^2s^{-1}
σ	electrical conductivity, sm^{-1}
ρ	density, kgm^{-3}
τ_w	wall shear stress, nm^{-2}
Subscripts	
Hnf	hybrid nanofluid
nf	nanofluid
f	fluid

1. Introduction:

Hybrid nanofluids, entailing of a base fluid and multiple types of nanoparticles, can significantly enhance heat transfer rates. When used in stretching sheet applications, the presence of nanoparticles in the fluid can enhance convective heat transfer from the sheet surface, leading to improved heat dissipation. This analysis of such flows helps in predicting and managing the behaviour of materials that exhibit viscoelastic characteristics, allowing for the design and optimization of processes and structures that involve these materials [1]. This research analysis the specific techniques and methods for nanoparticle incorporation into fluids can vary depending on the application and desired thermal performance. Further research and experimentation are continuously being conducted to optimize the design and application of nanoparticle-enhanced fluids for efficient heat transfer [2]. This research analysis of the Partial slip refers to the situation where the fluid velocity at the solid boundaries is not zero but rather has a non-zero slip velocity. This slip velocity introduces additional complexity to the enclosure's flow and heat transfer characteristics [3]. The equilibration dynamics occur on different timescales, depending on the specific properties of the system. For instance, collisional interactions between particles happen relatively quickly, resulting in particle agglomeration or separation explained by this analysis [4]. The integral treatment provides a simplified yet insightful approach to studying coupled heat and mass transfer from a radiating vertical thin needle in a porous medium. It allows for understanding the dominant mechanisms and provides useful engineering insights into the problem [5]. The study of diverse convection flow of SA-NaAlg-based MoS_2 nanofluids is aimed at understanding the enhanced heat transfer capabilities of nanofluids and exploring their potential applications in areas such as heat exchangers, cooling systems, and energy conversion devices [6]. Nanofluids, offer enhanced thermal, electrical, and mechanical characteristics compared to traditional fluids. These are just a few examples of the wide-ranging applications of nanofluids. As research and development in nanotechnology continue, new and exciting applications in various shapes and forms are likely to emerge in the future [7]-[10]. Hybrid nanofluids, which are a combination of nanoparticles and traditional base fluids, have gained significant attention in various fields due to their enhanced thermal conductivity and other favourable properties. When it comes to stretching sheet applications, hybrid nanofluids can offer several advantages. Here are a few potential applications of hybrid nanofluids in various geometrical shapes. The problem involves investigating the stream and heat transmission behaviour of the hybrid nanofluid under a

Casson-type fluid model with slip boundary conditions and sinusoidal heat circumstances [11]. This research analysis of the results of such simulations can help understanding the effects of each component and their interactions on the overall heat transfer and fluid flow behaviour [12]-[13]. This research investigates the applications in various fields, including heat exchangers, oil recovery processes, and magnetic drug targeting systems, where understanding the fluid behaviour and heat transfer is critical for optimization and design [14]-[15]. This research investigates understanding how the combination of these various factors affects the flow behaviour, heat transfer rates, and other fluid properties [16]. Due to the complexity of the problem investigating its solution, analysis, and interpretation would likely require expertise in fluid mechanics, heat transfer, magnetohydrodynamics, and nanofluid dynamics [17]. This analysis understands the thermodynamic behaviour of the system and optimizes heat transfer performance in applications such as porous media heat exchangers, cooling systems, or nanofluid-based heat transfer devices. The presence of viscoelastic behaviour and nanoparticle effects introduces additional complexities, making it an interesting area of research with practical implications [18]. Magnetohydrodynamics (MHD) is a branch of fluid dynamics that studies the behaviour of electrically conducting fluids in the presence of magnetic fields. It finds applications in various engineering and scientific fields, including metallurgy, astrophysics, and fusion research. In recent years, MHD has also been studied in the context of nanofluids, which are colloidal suspensions of nanoparticles in a base fluid. Some of the following research papers are considered here [19]-[23].

In this paper analysing the convective flow of a hybrid nanofluid with diverse base fluids over a stretching sheet involves the interaction of several physical phenomena, including the Lorentz force and viscous dissipation. The presence of the Lorentz force alters the fluid velocity distribution and flow patterns near the stretching sheet. This can lead to modifications in the boundary layer thickness and velocity profile, affecting the overall heat transfer rate. Viscous dissipation refers to the conversion of mechanical energy into heat due to the internal friction within the flowing fluid. The temperature rise due to viscous dissipation can alter the thermal boundary layer thickness, influencing the heat transfer rate between the fluid and the stretching sheet. Understanding these consequences is crucial in optimizing heat transfer processes in various engineering applications, such as cooling systems, heat exchangers, and thermal management of electronic devices.

2. Mathematical Formulation:

- In the presence of a uniform Lorentz force and viscous dissipation, deliberate stable, laminar, convective boundary layer flow along a stretching sheet in two dissimilar base fluids ((H_2O),($NaC_6H_9O_7$)) with two different hybrid nanoparticles (Titanium Oxide (TiO_2), Copper (Cu)).
- The study's goal would be to investigate the influence of hybrid nanoparticles, as well as the stuffs of magnetic fields and viscous dissipation, on the flow characteristics and heat transmission of the two base fluids.
- The presence of a magnetic field would introduce a Lorentz force term in the momentum equations and viscous dissipation in the energy equation, both of which would affect the flow behaviour.
- The surface temperature boundary condition would involve prescribing the temperature at the surface of the stretching sheet, which would affect the heat transfer characteristics of the system.
- The physical sketch of present model is shown in Fig.1.
- Beneath these assumptions, the governing equations in a stable state [11]

Continuity Equation:

$$\frac{\partial u}{\partial x}+\frac{\partial v}{\partial y}=0\,, \tag{1}$$

Momentum Equation:

$$u\frac{\partial u}{\partial x}+v\frac{\partial u}{\partial y}=\nu_{hnf}\left(1+\frac{1}{\beta}\right)\mu_{hnf}\frac{\partial^2 u}{\partial y^2}-\frac{\sigma_{hnf}}{\rho_{hnf}}B_0^2 u, \tag{2}$$

Energy Equation:

$$u\frac{\partial T}{\partial x}+v\frac{\partial T}{\partial y}=\frac{k_{hnf}}{(\rho C_p)_{hnf}}\frac{\partial^2 T}{\partial y^2}+\left(1+\frac{1}{\beta}\right)\frac{\mu_{hnf}}{(\rho C_p)_{hnf}}\left(\frac{\partial u}{\partial y}\right)^2 \tag{3}$$

Relevant boundary circumstances are

$$u=u_w=cx,\quad v=0,\quad T=T_w\quad at\quad y=0,$$
$$u=0,\quad T=T_\infty\quad at\quad y=\infty. \tag{4}$$

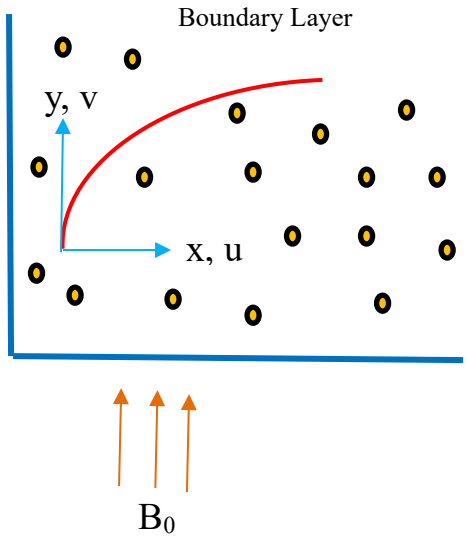

Fig.1 Stream of the problem

The hnf restrictions are given as

$$\mu_{hnf}=\frac{\mu_f}{(1-\phi_{np1})^{2.5}(1-\phi_{np2})^{2.5}}\,, \tag{5}$$

$$\rho_{hnf}=\{(1-\phi_{np2})[(1-\phi_{np1})\rho_f+\phi_{np1}\rho_{np1}]\}+\phi_2\rho_{np2}\,, \tag{6}$$

$$\alpha_{hnf}=\frac{k_{hnf}}{(\rho C_p)_{hnf}}\,, \tag{7}$$

$$(\rho C_p)_{hnf}=\left\{(1-\phi_{np2})\left[(1-\phi_{np1})(\rho C_p)_f+\phi_{np1}(\rho C_p)_{np1}\right]\right\}+\phi_{np2}(\rho C_p)_{np2}\,, \tag{8}$$

$$\frac{k_{hnf}}{k_{nf}}=\frac{k_{np2}+2k_{nf}-2\phi_{np2}(k_{nf}-k_{np2})}{k_{np2}+2k_{nf}+\phi_{np2}(k_{nf}-k_{np2})}\,, \tag{9}$$

where

$$\frac{k_{nf}}{k_f}=\frac{k_{np1}+2k_f-2\phi_{np1}(k_f-k_{np1})}{k_{np1}+2k_f+\phi_{np1}(k_f-k_{np1})}\,,$$
$$\frac{\sigma_{hnf}}{\sigma_{nf}}=\frac{\sigma_{np2}+2\sigma_{nf}-2\phi_{np2}(\sigma_{nf}-\sigma_{np2})}{\sigma_{np2}+2\sigma_{nf}+\phi_{np2}(\sigma_{nf}-\sigma_{np2})}, \tag{10}$$

where

$$\frac{\sigma_{nf}}{\sigma_f}=\frac{\sigma_{np1}+2\sigma_f-2\phi_{np1}(\sigma_f-\sigma_{np1})}{\sigma_{np1}+2\sigma_f+\phi_{np1}(\sigma_f-\sigma_{np1})}\,,$$

The suitable set of variables are

$$u = cxF'(\eta), \qquad v = -(cv)^{\frac{1}{2}} F(\eta), \quad \eta = \left(\frac{c}{\nu}\right)^{\frac{1}{2}} y, \qquad T - T_0 = (T_w - T_\infty)\theta(\eta), \tag{11}$$

Using above eqn. (11), eqns. (1) – (3) can be transmuted as,

$$\frac{\left(1+\frac{1}{\beta}\right)}{(1-\phi_{np1})^{2.5}(1-\phi_{np2})^{2.5}} F''' - \frac{\sigma_{hnf}}{\sigma_f} MF' + \left[(1-\phi_{np2})\left[1-\phi_{np1}+\phi_{np1}\frac{\rho_{np1}}{\rho_f}\right]+\phi_{np2}\frac{\rho_{np2}}{\rho_f}\right][FF''-F'^2] = 0, \tag{12}$$

$$\frac{k_{hnf}}{k_f}\frac{1}{Pr}\theta'' + \frac{Ec\left(1+\frac{1}{\beta}\right)}{(1-\phi_{np1})^{2.5}(1-\phi_{np2})^{2.5}} F''^2 + F\theta'\left[(1-\phi_{np2})\left[1-\phi_{np1}+\phi_{np1}\frac{(\rho C_p)_{np1}}{(\rho C_p)_f}\right]+\phi_{np2}\left(\frac{(\rho C_p)_{np2}}{(\rho C_p)_f}\right)\right] = 0, \tag{13}$$

and the related boundary restrictions are

$$F(0) = 0, \quad F'(0) = 1, \quad \theta(0) = 1,$$
$$F'(\infty) = 0, \quad \theta(\infty) = 0 \tag{14}$$

where,

$$M = \frac{\sigma_f B_0^2}{c\rho_f}, \qquad Pr = \frac{\nu_f}{\alpha_f}, \quad Ec = \frac{c^2x^2}{C_{p_f}}\,(T_w - T_\infty) \tag{15}$$

2.1 Nusselt number and Skin friction Analysis:

The dimensionless form of C_f and Nu, are

$$C_f = \frac{\tau_w}{\rho_f u_w^2}, \quad Nu = \frac{xq_w}{k_f(T_w - T_\infty)} \tag{16}$$

$$\tau_w = \mu_{hnf}\left(1+\frac{1}{\beta}\right)\left(\frac{\partial u}{\partial y}\right)_{y=0}, \quad q_w = -k_{hnf}\left(\frac{\partial T}{\partial y}\right)_{y=0} \tag{17}$$

$$NuRe^{-1/2} = -\left(\frac{k_{hnf}}{k_f}\right)\theta'(0). \tag{18}$$

$$C_f Re^{1/2} = \left(1+\frac{1}{\beta}\right)\left(\frac{\mu_{hnf}}{\mu_f}\right)F''(0) \tag{19}$$

3. Solution Procedure :

The resulting ordinary differential equations expressed in Eqns. (12) & (13) restricted to the boundary restraints (14) have been resolved by IVth order Runge-Kutta form with shooting manner with the support of BVP4C code in MATLAB software. We indicate $F = y_1,\ \theta = y_4$ for our present model and render a prime step of the system are:

$$y_1' = y_2$$
$$y_2' = y_3$$
$$y_3' = \left(1+\frac{1}{\beta}\right)^{-1}\left((1-\phi_{np1})^{2.5}(1-\phi_{np2})^{2.5}\right)\left\{\frac{\sigma_{hnf}}{\sigma_f}My_2 - \left[(1-\phi_{np2})\left[1-\phi_{np1}+\phi_{np1}\frac{\rho_{np1}}{\rho_f}\right]+\phi_{np2}\frac{\rho_{np2}}{\rho_f}\right][y_1y_3 - y_2^2]\right\}$$
$$y_4' = y_5$$

$$y_5' = -Pr\frac{k_f}{k_{hnf}}\left\{\frac{Ec\left(1+\frac{1}{\beta}\right)}{\left(1-\phi_{np1}\right)^{2.5}\left(1-\phi_{np2}\right)^{2.5}}{y_3}^2 + \left[\left(1-\phi_{np2}\right)\left[1-\phi_{np1}+\phi_{np1}\frac{\left(\rho C_p\right)_{np1}}{\left(\rho C_p\right)_f}\right]+\phi_{np2}\left(\frac{\left(\rho C_p\right)_{np2}}{\left(\rho C_p\right)_f}\right)\right][y_1 y_5]\right\}$$

and

$y_1(0) = 0,\ y_2(0) = 1,\ y_4(0) = 1$

The initial estimates were given to $y_3(0)$ i.e., $F''(0)$ and $y_5(0)$ i.e., $\theta'(0)$. Then initial guesstimates were then conveniently modified to satisfy the boundary requirement and the convergence criterion of 10^{-6}.

4. Review and Discussion of the Results:

Figure 1 depict the items are placed of the conundrum. In regard to physical behaviour and attitude are explained in the Figures 2-9 have been drawn for the hybrid nanofluid flow, which consists of TiO_2 and Cu nanoparticles, (H2O, and $NaC_6H_9O_7$) are considered as base fluids to demonstrate the impression of numerous parameters on acceleration, thermal profiles.

4.1 Velocity Profile:

Fig.2.explains, when a magnetic field ($M = 1,3,5$) is applied to a flowing fluid, it can induce changes in the flow behavior due to the interaction between the magnetic field and the fluid's properties. This phenomenon is known as magnetohydrodynamics (MHD). The effect of a magnetic field on the velocity profile in a stretching sheet flow depends on the fluid's conductivity and its response to magnetic forces. When water is used as the base fluid, the magnetic field has a negligible effect on the velocity profile in the stretching sheet flow. However, when sodium alginate is employed, the magnetic field induces a Lorentz force that alters the flow behaviour, resulting in a velocity profile decrease in the fluid velocity near the stretching sheet.

As the Eckert number increases ($Ec = 1,3,5$), the velocity profile in the stretching sheet tends to decrease. This is because higher Eckert numbers correspond to a stronger convective heat transfer effect, which results in increased thermal energy near the surface of the sheet. This additional energy leads to a decrease in the fluid's velocity. When (H_2O, and $NaC_6H_9O_7$) are used as the base fluids, sodium alginate is typically added as a thickening agent. It increases the fluid's viscosity and can affect the velocity profile. Higher viscosity generally results in lower fluid velocities, especially near the surface of the stretching sheet. Therefore, when sodium alginate is added, the velocity profile is expected to decrease even more compared to using water alone as explained in Fig.3.

As the concentration of titanium oxide nanoparticles increases, it typically mains to an intensification in the viscosity of the fluid in Fig. 4. Higher viscosity implies greater resistance to flow, affecting the stretching sheet's velocity profile. Due to the increased viscosity, the fluid near the surface of the sheet experiences more drag, resulting in a reduced velocity at that location. This reduction in velocity is likely to be more pronounced near the sheet's surface, gradually transitioning to the base fluid's velocity farther away from the sheet.

As the Casson parameter upsurges, the maximum velocity in the fluid flow decreases. This reduction occurs because higher Casson parameters indicate higher viscosity and resistance to flow. Consequently, the fluid experiences greater resistance while stretching, resulting in a decrease in the maximum velocity as appeared in Fig .5.

4.2 Thermal Profile:

As the magnetic field strength increases in a stretching sheet with water and sodium alginate as base fluids, the temperature profile can be increased by changes in fluid flow patterns, and alterations in thermal conductivity in Fig. 6. The precise details of the temperature profile will depend on the specific parameters of the system, such as the magnetic field strength, stretching velocity, fluid properties, and boundary conditions.

When water or sodium alginate is used as the base fluid in a stretching sheet flow, an increase in the Eckert number generally results in a higher temperature profile near the stretching sheet. As the Eckert number intensifications, the kinetic energy of the fluid flow becomes more significant, resulting in higher energy conversion into thermal energy near the stretching sheet. The presence of sodium alginate can affect heat transfer characteristics due to its rheological properties, such as viscosity and elasticity. These properties can influence the flow behaviour and heat transfer mechanisms, leading to deviations from the temperature profile observed with water as the base fluid as exposed in Fig.7.

As the concentration of titanium oxide and copper nanoparticles increases in water and sodium alginate base fluids, the thermal conduction and thickness of the fluid can be affected in Fig. 8. This, in turn, can impact the temperature profile in the stretching sheet, potentially leading to higher temperatures.

Due to the augmented heat transfer, the temperature near the stretching surface tends to decrease with an increasing Casson parameter. The stronger resistance to flow prevents the fluid from retaining heat near the sheet, resulting in a more efficient cooling effect. Therefore, as the Casson parameter increases, the temperature near the stretching sheet decreases in Fig.9.

4.3 Velocity Distributions:

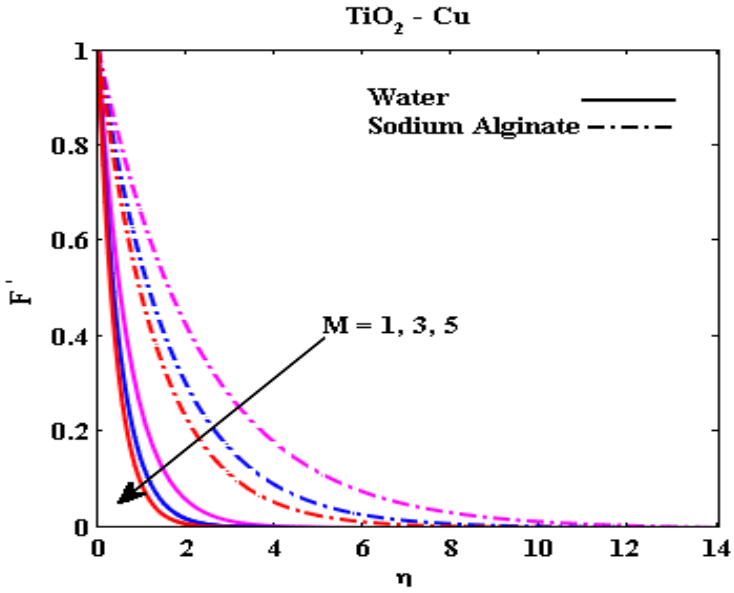

Fig. 2. The impacts of $M = 1,3,5$ on f'.

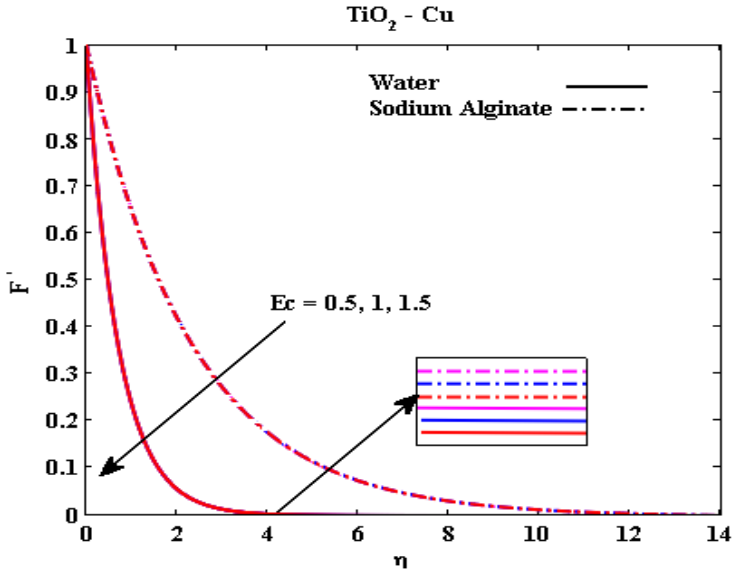

Fig. 3. The impacts of $Ec = 0.5,1,1.5$ on f'.

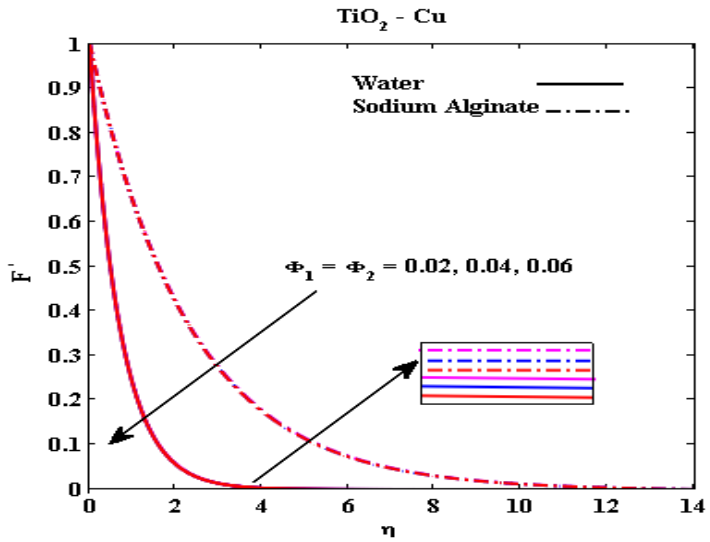

Fig. 4. The impacts of $\varphi_1 = \varphi_2 = 0.02,0.04,0.06$ on f'.

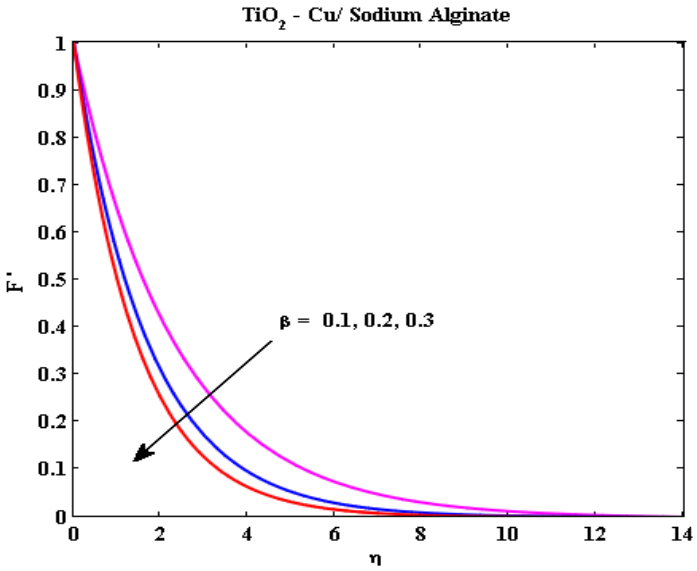

Fig. 5. The impacts of $\beta = 0.1,0.2,0.3$, on f' .

4.4 Temperature Distributions:

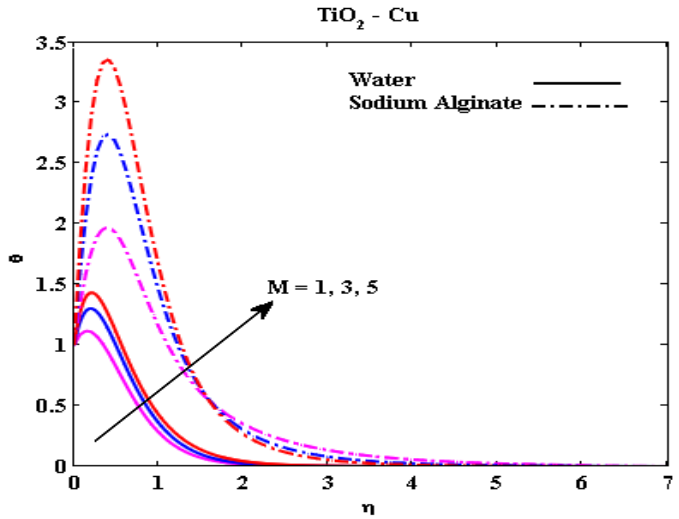

Fig. 6. The impacts of $M = 1,3,5$ on θ

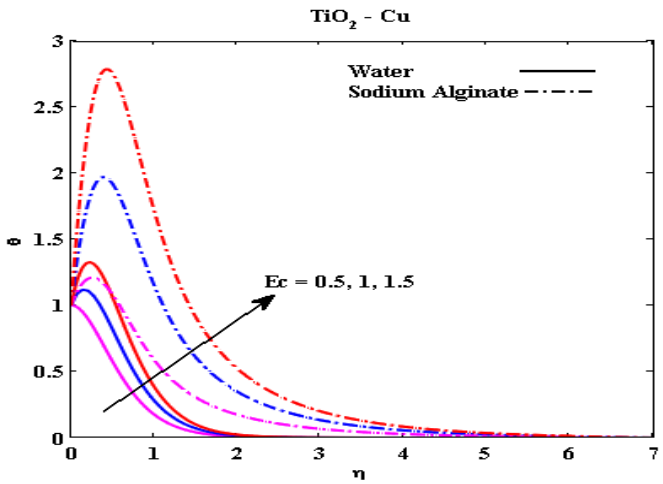

Fig. 7. The impacts of $Ec = 0.5,1,1.5$ on θ

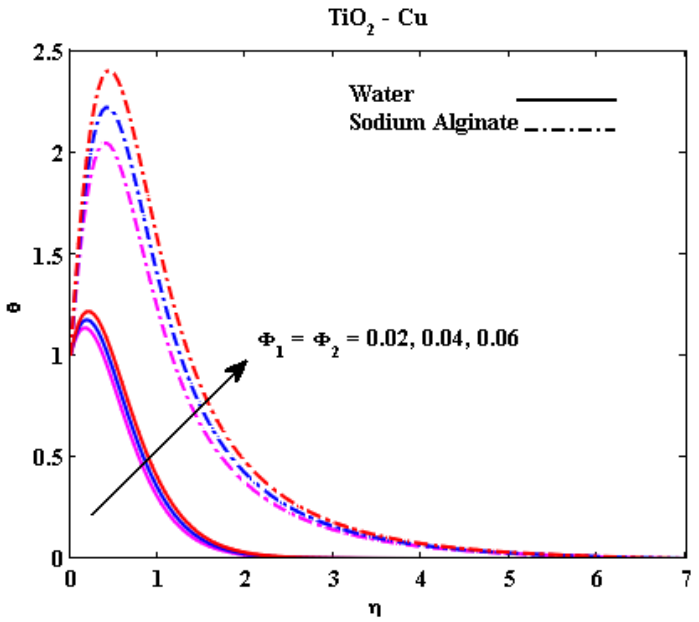

Fig. 8. The impacts of $\varphi_1 = \varphi_2 = 0.02,0.04,0.06$ on θ.

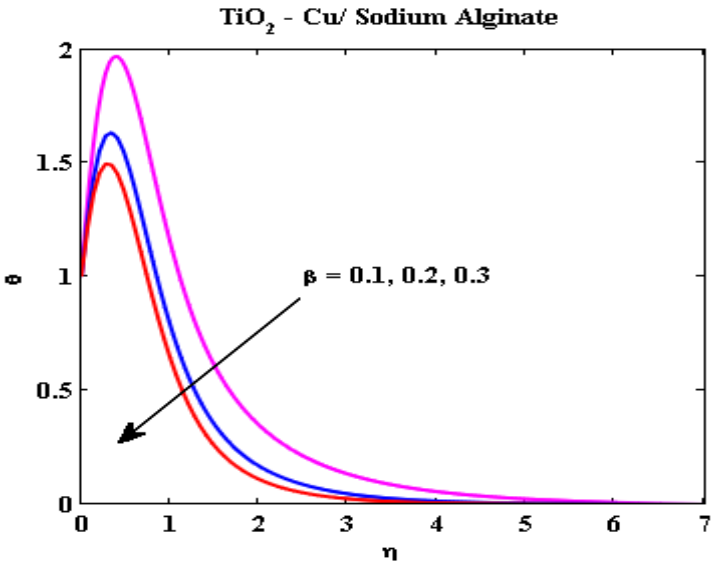

Fig. 9. The impacts of $\beta = 0.1,0.2,0.3$ on θ.

Table 1: Thermophysical appearances of the base fluids and the nanoparticles

Base fluid and nanoparticle	C_p/(J/(kg.K))	ρ/(kg/m^3)	k/(W/(m.K))	σ(sm^{-1})
H_2O	4179	997	0.613	0.05
$NaC_6H_9O_7$	4175	989	0.6376	$2.6x10^{-4}$
TiO_2	686.2	4250	8.954	$2.38x10^{6}$
Cu	385	8933	400	$5.96x10^{7}$

Table 2: **The values of C_f coefficient and Nu for M, β with surface temperature is listed below**

M	Ec	β	$C_f Re^{1/2}$		$Nu Re^{-1/2}$	
			TiO_2 - Cu		TiO_2 - Cu	
			H_2O	$NaC_6H_9O_7$	H_2O	$NaC_6H_9O_7$
1	1	0.1	-1.5162	-5.8974	-1.7405	-9.6040
3			-2.1197	-7.4477	-3.6869	-12.6109
5			-2.5870	-8.8068	-5.2449	-15.6369
1	0.5	0.1	-1.5162	-5.8974	-0.0203	-3.8231
	1		-1.5162	-5.8974	-1.7405	-9.6040
	1.5		-1.5162	-5.8974	-3.4608	-15.3849
1	1	0.1	-	-5.8974	-	-9.6040
		0.2	-	-3.9793	-	-5.8715
		0.3	-	-3.2847	-	-4.6240

5. Conclusions:

In the conclusion part of the study on the convective flow of a hybrid nanofluid with diverse base fluids in heat transmission over a stretching sheet, summarized their findings and discussed the consequences of incorporating the Lorentz force and viscous dissipation. The following outcomes and consequences have been discussed:

5.1 Enhanced heat transfer: The inclusion of nanoparticles in the base fluid (nanofluid) could have led to enhanced heat transfer properties. The Lorentz force, which arises due to the existence of a magnetic field, might have contributed to better fluid mixing and heat distribution, leading to improved heat transmission rates. This effect could be beneficial for various industrial applications where efficient heat transfer is crucial.

5.2 Control of boundary layer behaviour: The Lorentz force might have influenced the behaviour of the boundary layer near the stretching sheet. By controlling the boundary layer, the researchers may have observed fluctuations in the flow pattern and heat transmission characteristics, leading to potential improvements in heat transfer performance.

5.3 Influence of nanoparticle type: The use of different types of nanoparticles in the hybrid nanofluid could have resulted in varying heat transfer behaviours. Some nanoparticles might have exhibited better thermal conductivity, while others could have had a stronger impact on the fluid flow due to their magnetic properties.

5.4 Viscous dissipation effects: Viscous dissipation refers to the energy conversion from kinetic energy to thermal energy within the fluid due to the presence of viscous forces. The researchers might have analysed the consequences of viscous dissipation in the context of heat transmission over the stretching sheet.

The above points provide a general overview of the possible outcomes and implications that could have been presented in the conclusion section of the research paper.

6. References:

1. N.J. Balmforth, R.V. Craster, A.C. Rust and R. Sassi, Viscoplastic flow over an inclined surface, J. Non-Newtonian Fluid Mech., 139 (2006) 103–127.
2. S.U.S. Choi and J.A. Eastman, Enhancing thermal conductivity of fluids with nanoparticles, ASME Int. Mech. Eng. Congress. Exposition, (1995) 12-17.
3. A.J. Chamkha, A.M. Rashad, T. Armaghani and M.A. Mansour, Effects of partial slip on entropy generation and MHD combined convection in a lid-driven porous enclosure saturated with a Cu-water

nanofluid, J. Thermal Analy. Calorimetry, 132 (2) (2018) 1291-1306. http://dx.doi.org/10.1007/s10973-017-6918-8.

4. J. Wong, M. Lindstrom and A.L. Bertozzi, Fast equilibration dynamics of viscous particle-laden flow in an inclined channel, J. Fluid Mech., 879 (2019) 28-53. Doi:10.1017/jfm.2019.685.
5. N. Bano and B.B. Singh, An integral treatment for coupled heat and mass transfer by natural convection from a radiating vertical thin needle in a porous medium, Int. Communi. Heat. Mass Transf., 84 (2017) 41-48. http://dx.doi.org/10.1016/j.icheatmasstransfer.2017.03.007.
6. T.N. Ahmed and I. Khan, Mixed convection flow of sodium alginate (SA-NaAlg) based molybdenum disulphide (MoS2) nanofluids: Maxwell Garnetts and Brinkman models, Res. Phys., 8 (2018) 752-757. Doi: https://doi.org/10.1016/j.rinp.2018.01.004.
7. I.S. Oyelakin, S. Mondal and P. Sibanda, Unsteady Casson nanofluid flow over a stretching sheet with thermal radiation, convective and slip boundary conditions, Alexandria Eng. J., 55 (2016) 1025–1035. Doi: http://dx.doi.org/10.1016/j.aej.2016.03.003.
8. M. Hatami and D. D. Ganji, Natural convection of sodium alginate (SA) non-Newtonian nanofluid flow between two vertical flat plates by analytical and numerical methods, Case Studies. Thermal Eng., 2 (2014) 14-22. Doi: http://dx.doi.org/10.1016/j.csite.2013.11.001.
9. Z. Iqbal, S. Yashodha, A. K. Abdul Hakeem, A. Alsawi, M.A. Alyami, E.S. Yousef., A.H. Amin and S.M. Eldin, 2022.Energy transport analysis in natural convective flow of water: Ethylene glycol (50:50)-based nanofluid around a spinning down-pointing vertical cone. Front. Mater., 9 (2022) 1037201. Doi: 10.3389/fmats.1037201.
10. M.V.S. Rao, K. Gangadhar and A. Srinivasa Rao, Exact and numerical solutions for MHD boundary layer flow of Casson fluid over a stretching sheet, Int. J. Eng. Adv. Tech., 9 (2019) 2249-8958. Doi: 10.35940/ijeat.A1053.1291S52019.

A. Raza, M.Y. Almusawa, Q. Ali, A. U. Haq, K. A. Khaled and I.E. Sarris, Solution of water and sodium alginate-based Casson type hybrid nanofluid with slip and sinusoidal heat conditions: a Prabhakar fractional derivative approach, Symmetry, 14 (2022) 2658. Doi: https://doi.org/10.3390/sym14122658.

A. Hussanan., M. Qasim and Z. M. Chen, Heat transfer enhancement in sodium alginate based magnetic and non-magnetic nanoparticles mixture hybrid nanofluid, Physica A, 550 (2020) 123957. Doi: https://doi.org/10.1016/j.physa.2019.123957.

11. A.J. Chamkha, A.M. Rashad, T. Armaghani, M.A. Mansour and M. Ghalamba, 2017. Effects of heat sink and source and entropy generation on MHD mixed convection of a Cu-water nanofluid in a lid-driven square porous enclosure with partial slip, Phys. Fluids, 29 (2017) 052001. Doi: 10.1063/1.4981911.
12. N. Indumathi, B. Ganga, S. Charles and A.K. Abdul Hakeem, Magnetohydrodynamics boundary layer flow past a wedge of Casson CuO-TiO_2/EG embedded in non-Darcian porous media: viscous dissipation effects. J. Nanofluids 11 (2022) 906-914.
13. A.K.W. Loh, G.M. Chen and B.K. Lim, Viscous dissipation effect on forced convective transport of nanofluids in an asymmetrically heated parallel-plate microchannel, Case Studies. Thermal Eng., 35 (2022) 102056 Doi: https://doi.org/10.1016/j.csite.2022.102056.

A. Mahdy, E.R. El-Zahar, A.M. Rashad, W. Saad and H.S. Al-Juaydi The magneto-natural convection flow of a micropolar hybrid nanofluid over a vertical plate saturated in a porous medium, Fluids, 6 (6) (2021) 202. Doi: https://doi.org/10.3390/fluids6060202.

14. E.R. El-Zahar, A. Mahdy, A.M. Rashad and W. Saad, Unsteady MHD mixed convection flow of non-Newtonian Casson hybrid nanofluid in the stagnation zone of sphere spinning impulsively, Fluids, 6 (6) (2021) 197. Doi: https://doi.org/10.3390/fluids6060197
15. T. Gul, S. Mukhtar, W. Alghamdi, I. Ali, A. Saeed and P. Kumam, Entropy and Bejan number influence on the liquid film flow of viscoelastic hybrid nanofluids in a porous space in terms of heat transfer, ACS Omega, 7 (2022) 33365-33374. https://doi.org/10.1021/acsomega.2c03975.
16. T. Sravan Kumar, Hybrid nanofluid slip flow and heat transfer over a stretching surface, Partial Diff. Eqns. Applied Math., 4 (2021) 100070.
17. S. Reddy, P. Sreedevi and A.J. Chamkha, Hybrid nanofluid heat and mass transfer characteristics over a stretching/shrinking sheet with slip effects, J. Nanofluids 12 (2023) 251–260.
18. T. Armaghani, M.S. Sadeghi, A.M. Rashad, M.A. Mansour, A.J. Chamkha, A.S. Dogonchi, A. Hossam and Nabwey, MHD mixed convection of localized heat source/sink in an Al_2O_3-Cu/water hybrid nanofluid in lid-shaped cavity, Alexandria Eng. J., 60 (3) (2021) 2947-2962. Doi: https://doi.org/10.1016/j.aej.2021.01.031.
19. P. Bitla and F.Y. Sitotaw, Effects of slip and inclined magnetic field on the flow of immiscible fluids (couple stress fluid and Jeffrey fluid) in a porous channel, J. Applied Math., (2022) 2799773. Doi: https://doi.org/10.1155/2022/2799773.
20. A.M. Rashad, A.J. Chamkha, A. Muneer, Ismael and T. Salah, Magnetohydrodynamics natural convection in a triangular cavity filled with a Cu- Al_2O_3/water hybrid nanofluid with localized heating from below and internal heat generation, J. Heat Transf., 140 (7) (2018) 072502-072513. Doi: https://doi.org/10.1115/1.4039213.